ACES Asian Chemical Editorial Society

DOI: 10.1002/asia.201901512

CHEMISTRY AN ASIAN JOURNAL Communicatio

Label-Free Detection of Transferrin Receptor by a Designed Ligand-Protein Sensor

Wanshan Liu, Shiyu Sun, Yida Huang, Ruimin Wang, Jiale Xu, Xiyuan Liu, and Kun Qian*[a]

Abstract: Advanced detection of biomarkers in biofluids plays an important role in disease diagnosis and prognosis. Current techniques with pre-labelling suffer from high cost and complicated operation, etc. Herein, we designed a label-free electrochemical biosensor for rapid detection of transferrin receptor with desirable linear range, sensitivity, specificity, reproducibility, and stability for practical applications.

Biomarker proteins in biofluid systems are widely used for biological research and clinical analysis, since their expression levels directly reflect the physiological status and disease progression.[1] Especially, the detection of certain biomarker proteins in serum (e.g., transferrin receptor, TFR) has been demonstrated as an effective manner in disease diagnosis and prognosis, with high sensitivity and specificity.[1a,2] However, due to the low abundance of biomarkers and high complexity of biosystems, quantitative detection of biomarkers is still challenging in real case biosamples.[3] To date, it is always in demand to construct new platforms for biomarker detection toward practical applications.

The specific bonding with target molecules is universally required in clinical detection of biomarkers.[1c,4] The conventional labelling approach such as immunoassay is based on antibody-antigen recognition, which suffers from I) low accuracy of measurement due to labelling;[5] II) high cost of antibody and related reagents;[5,6] III) complex and time-consuming operation;[5b,7] and IV) susceptibility to environment (such as temperature and light).[8] Considering above aspects, label-free detection with ligand-protein binding is desirable as an emerging choice of molecular recognition, owing to its stability and easy accessibility.[2b,9] For example, specific combination between transferrin (TF) and TFR can be applied to quantitation and imaging, which may characterize diseases such as anemia and cancer.[10] Notably, such type of interaction is limited and few reported in electrochemical sensing, with high precision and low cost.[10c,11] Furthermore, label-free method without pre-labelling process represents the next-generation tool for its simple procedures and requires smart design for practical use.[12] Hence, label-free electrochemical detection based on ligand-protein binding may contribute to novel high-efficacy sensors toward disease diagnostics.

Herein, we proposed a label-free electrochemical sensor for TFR detection through ligand-receptor binding (Scheme 1). The biosensor was fabricated through layer-by-layer deposition method. We functionalized chitosan (Chi) on the indium tin oxide (ITO) electrode to form a positively charged layer and then assembled multi-walled carbon nanotubes in conjugation with transferrin (MWCNTs-TF, negatively charged). The prepared sensor afforded a linear range in TFR detection (1–10000 ng mL^{-1}) and the limit-of-detection (LOD) reached 0.082 ng mL^{-1}, comparable with the best current results. We also demonstrated the high specificity, reproducibility, and stability of sensors for biomarker detection. This work would contribute to the development of platforms for TFR detection and the design of ligand-based approaches for label-free analysis of serum biomarkers in diagnostic applications.

The electrochemical biosensor was constructed through layer-by-layer assembling (Scheme 1). The bare ITO showed roughness caused by ITO nanoparticles (Figure 1a) according to scanning electron microscopy (SEM). After dropping the chitosan solution, a uniform layer was formed with positive charges (Figure S1a), acting as a medium between negatively charged ITO electrode[13] and further assembling layer. MWCNTs-TF with negative charges was then deposited and showed enhanced surface roughness (Figure S1b). Blocking by bovine serum albumin (BSA) didn't affect the surface morphology (Figure 1b), agreed to the previous results.[14] Atomic force microscopy (AFM) results confirmed the change of roughness, with the root-mean square (rms) roughness changing from ≈4.46 nm to ≈21.86 nm during the whole process (Figure 1c&d, Figure S1c&d). Furthermore, static contact angle analysis was conducted to examine the assembly process from triple replicate measurements (Figure 1e). The contact angle decreased from 81.6±0.6° to 63.0±4.1° due to the hydrophilicity of carboxylated multi-walled carbon nanotubes (MWCNTs-COOH)[15] and then increased to 72.8±3.5° due to the hydrophobicity of BSA.[16] Also, zeta potentials of materials were measured in Figure 1f, consistent with other characterizations on the layer-by-layer assembling. All above data demonstrated the successful modification on the surface of electrodes and the construction of biosensors.

Differential pulse voltammetry (DPV) and cyclic voltammetry (CV) curves were recorded to characterize electrochemical sensing of electrodes (Figure S2). For DPV curves (Figure 2a), bare ITO afforded a reduction current peak of 8.68±0.22 μA. After the modification of chitosan, the current peak increased to 20.6±0.94 μA (p-value < 0.001) and loading of MWCNTs-TF induced a further increase to 29.7±0.78 μA (p-value < 0.001),

[a] W. Liu, S. Sun, Y. Huang, R. Wang, J. Xu, X. Liu, Prof. K. Qian
School of Biomedical Engineering
Shanghai Jiao Tong University
Shanghai 200030 (P. R. China)
E-mail: k.qian@sjtu.edu.cn

Supporting information and the ORCID identification number(s) for the author(s) of this article can be found under:
https://doi.org/10.1002/asia.201901512.

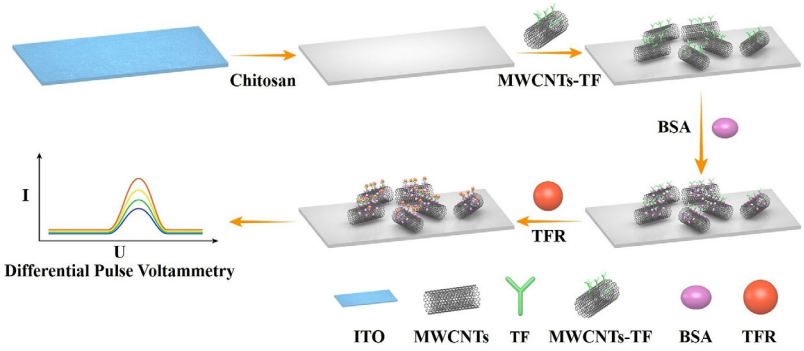

Scheme 1. The overall schematics showing fabrication of ITO-Chi-MWCNTs-TF-BSA biosensor and electrochemical detection of TFR.

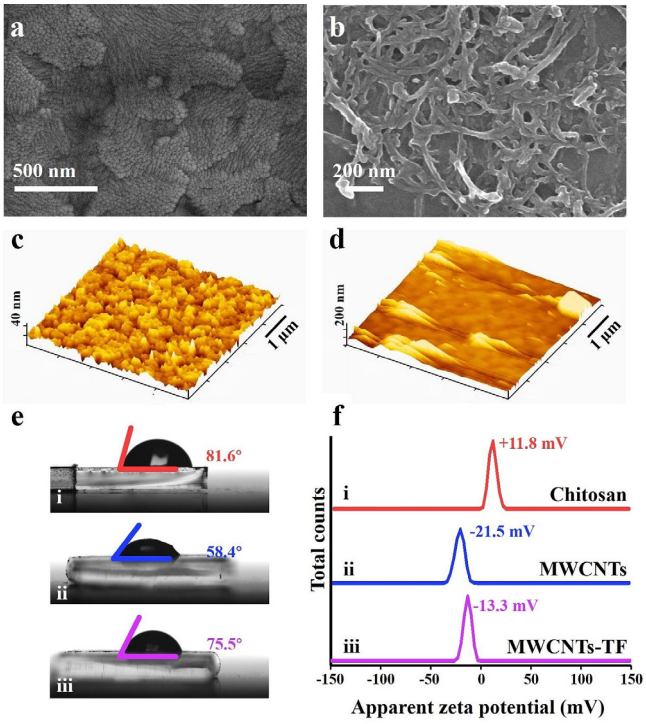

Figure 1. Characterization of materials. SEM images of a) bare ITO electrode, b) prepared electrochemical sensor (ITO-Chi-MWCNTs-TF-BSA); AFM images of c) bare ITO electrode, d) prepared electrochemical sensor (ITO-Chi-MWCNTs-TF-BSA). The values of rms roughness were c) ≈4.46 nm and d) ≈21.86 nm. e) Contact angle of i) bare ITO, ii) ITO-Chi-MWCNTs-TF, and iii) ITO-Chi-MWCNTs-TF-BSA; and f) zeta potential of i) chitosan, ii) MWCNTs, and iii) MWCNTs-TF.

due to the high conductivity of carbon nanotubes.[17] Binding of BSA caused a decrease of current peak to 27.6 ± 0.25 μA (p-value < 0.005), due to the low electric conductivity of BSA.[17,18] Notably, the electronic conductivity was enhanced by 3.18-fold (p-value < 0.001) through the whole process of biosensor fabrication. The current responses in CV curves (Figure 2b) showed the similar results with DPV and the statistical analysis of DPV current peaks by five independent experiments was showed with error bars in Figure 2c. Consequently, we concluded the high reproducibility of the sensor through serial electrochemical measurements.

After incubation of TFR, the value of current peak decreased and the current change reflected the combined quantity of TFR (Figure 3a). The device construction was shown in Figure S3. Before detecting the standard curve of TFR solutions and serum samples, pH, temperature, and time of incubation were optimized for later biosensing. As displayed in Figure 2d&e, current peaks appeared at pH of 7.0 and temperature of 37 °C, showing the optimized condition similar to the normal physiological state. Besides, with the increased incubation time, the current response became stable when the time was over 30 min (Figure 2f), indicating that 30 min could be the optimized condition for the TF/TFR incubation. These optimizations of the sensor were critical for the next application tests.

Specifically, the DPV curves of different concentrations (1–10 000 ng mL^{-1}) of TFR were measured using the optimized conditions above. The current responses decreased as the TFR concentration increased (Figure 3a), showing a linear regression equation of I (μA) = −1.47 × log (concentration$_{TFR}$) + 25.3 and a correlation coefficient of 0.99 (Figure 3b). According to the regression plot, the LOD was calculated to be 0.082 ng mL^{-1} (signal-to-ratio of 3) and corresponding current value (26.90 μA) was the mean of the blank control minus 3 times of its standard deviations.[4a,b,17] The mean and standard deviation of the blank control were calculated from 3 independent experiments. The high accuracy, low LOD, and wide linear range of TFR measurement demonstrated the potential for clinical use.[10a,b,19] We also detected TFR in serum with different dilutions (10^0, 10^1, 10^2, 10^3-fold). The values of current peaks increased as the serum diluted (Figure S4). In addition, we verified specificity, reproducibility, and stability of the biosensor. For specificity, the current change for exclusive TFR was approximate to the results of TFR mixed with other molecules, showing the high selectivity of the biosensor (Figure 3c). For reproducibility, the current peaks of standard solutions had low variations (≈5.0%), suggesting high inter-biosensor reproducibility (Figure S5). For stability, the same biosensor afforded stable performance (peak variation < 1%) after the storage at 4 °C for 3 and 6 days (Figure 3d). Notably, the high performance of the sensor in this work could be comparable to the best current results[2b,17,20] and further application in serum

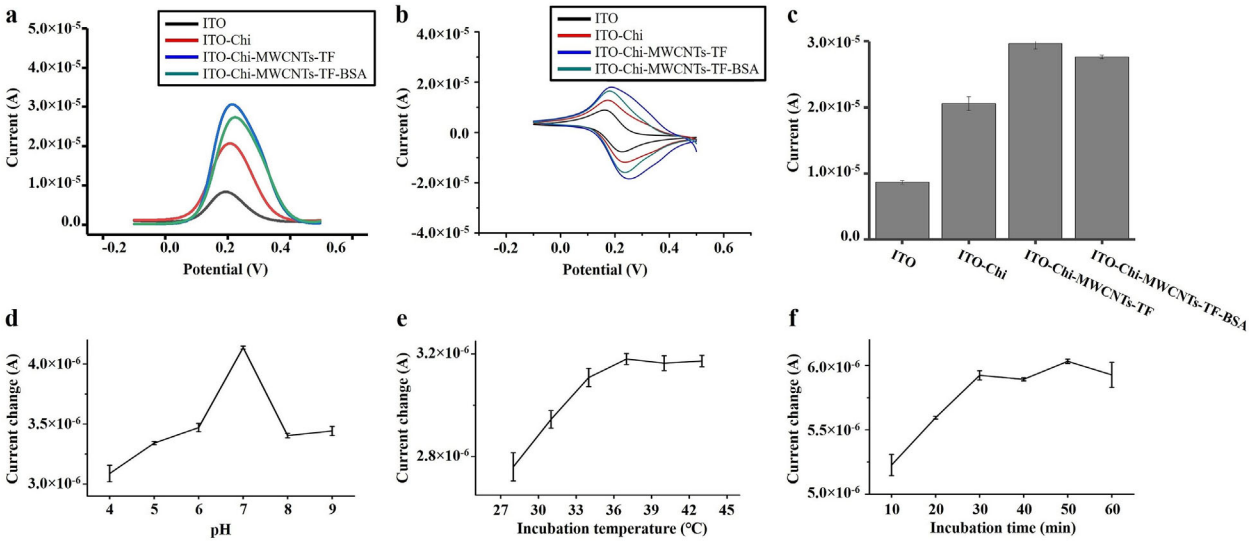

Figure 2. Electrochemical sensing and optimization. Typical a) DPV and b) CV curves of bare ITO, ITO-Chi, ITO-Chi-MWCNTs-TF, and ITO-Chi-MWCNTs-TF-BSA; c) average values of DPV current peaks of ITO, ITO-Chi, ITO-Chi-MWCNTs-TF and ITO-Chi-MWCNTs-TF-BSA. The means and error bars were calculated from 5 replicate measurements. Current change of biosensors under different d) pH, e) incubation temperature, and f) TF/TFR incubation time using 100 ng mL^{-1} TFR solutions.

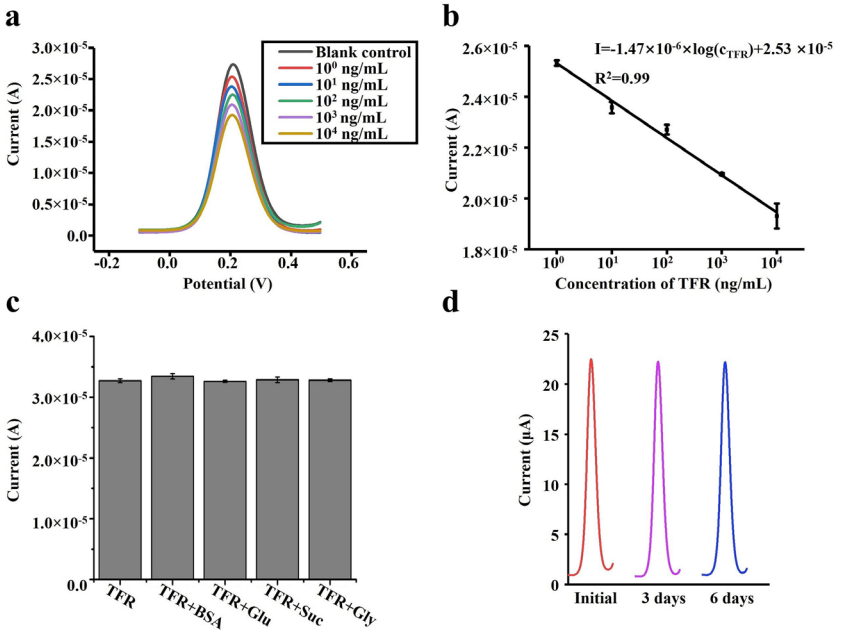

Figure 3. Detection of TFR. a) Typical DPV curves and b) regression plot of standard TFR solutions with different concentrations ranging from 1–10 000 ng mL^{-1} by triple independent tests; c) specific testing of biosensor using TFR, TFR + BSA, TFR + glucose (Glu), TFR + sucrose (Suc), TFR + glycine (Gly); and d) the current responses of biosensor after storage at 4 °C for 0, 3, and 6 days. Standard solutions for incubation contained BSA, glucose, sucrose, and glycine (each at a concentration of 100 ng mL^{-1}) in c). All standard solutions contained 100 ng mL^{-1} TFR in c) and d).

analysis displayed the strong potential of the sensor in clinical laboratory.

Moreover, standard TFR solutions were tested by enzyme-linked immunosorbent assay (ELISA), demonstrating the advantages of electrochemical biosensor further. As the regression plot (Figure S6), there was a polynomial relationship between concentrations of TFR and optical density at 450 nm (OD450), and LOD was 75.7 ng mL^{-1}. Compared with ELISA, the biosensor afforded i) wider linear range and lower LOD; ii) less time consumed (electrochemical biosensor: only ≈1 min for single DPV curve and ≈35 min for incubation and DPV measurements for 3 times; ELISA: ≈100 min); and iii) lower cost of only ≈0.2 RMB for each biosensor without labor costs, including the bare ITO electrode (≈0.14 RMB each) and other reagents (≈0.04 RMB for one prepared electrode), supporting for large-scale application.

In summary, we built a new label-free electrochemical biosensor (ITO-Chi-MWCNTs-TF-BSA) based on ligand-protein in-

teraction with high-performance detection of TFR. The sensor enjoyed the following major advantages: 1) capture of TFR by TF in a label-free manner; 2) optimized performance with wide linear range of 1–10 000 ng mL^{-1}, LOD of 0.082 ng mL^{-1}, as well as high specificity, reproducibility, and stability; and 3) real case application in serum samples with less time, low cost and ideal performance.

We anticipate several research lines following this work, in the field of material development, analyte exploration, and clinical analysis. For material development, design of bio-material interface would improve the performance of the sensor further. For analyte exploration, more analytes could be detected with selected probes and methods. For clinical analysis, the sensor might be applied to other application scenarios. As the merits and directions are demonstrated above, we hope that our approach may not only serve as a versatile platform for specific biomarker detection and analysis but also increase the application of electrochemical sensors in diagnostic applications.

Experimental Section

Synthesis of MWCNTs-TF. Carboxylated multi-walled carbon nanotubes (MWCNTs-COOH) and transferrin were linked to form MWCNTs-TF through 3-(3-dimethylaminoprophyl)-1-ethylcarbodiimide hydrochloride (EDC)/*N*-hydroxysuccinimide (NHS) reaction.[12c,21] In order to activate carboxyl groups, MWCNTs-COOH (12 mg, Chengdu Organic Chemicals Co. Ltd., Chinese Academy of Sciences) were mixed with EDC (4.4 mg, 99%), NHS (3.2 mg, 98%) and Triton X-100/water solution (24 mL, 0.3% by V V^{-1}),[18,21a,22] followed by ultrasonicated for 1 h and stirred for 4 h at room temperature. Whereafter, 12 mg transferrin (ProSpec company, Israel) was added into the solution. After stirred in the ice for 1 h and kept at 4 °C for over 20 h, the prepared MWCNTs-TF was centrifuged for 10 min (4 °C, 8000 × g) and washed with deionized water for three times. The final MWCNTs-TF were dispersed in 24 mL of Triton X-100/HCl solution (0.3% by V/V, pH of HCl solution = 5.0) and stored at 4 °C for later use.

Preparation of biosensors. The biosensor was fabricated through layer-by-layer deposition method. The bare ITO electrode (25 mm × 7.5 mm × 1.1 mm, 5–7 Ω, Luoyang Tengchang Xukun Biotechnology) was divided into three regions by insulating membrane. The ITO electrode was cleaned with ultrasonic washer in ethanol, acetone, 2-propanol, and deionized water alternately and dried before use. Then, chitosan was dispersed in acetate buffer (pH 3.0)[17,23] and 40 μL of chitosan solution (0.5 mg mL^{-1}) was dropped onto the ITO electrode and dried at 50 °C to form a thin chitosan layer (positively charged). Subsequently, 20 μL of MWCNTs-TF solution (negatively charged) was deposited onto chitosan layer and dried naturally for 1 h. Afterwards, the electrode was incubated in 0.1% bovine serum albumin (BSA) solution for 30 min for blocking.[14,24] The final ITO-Chi-MWCNTs-TF-BSA biosensor was washed with deionized water and stored at 4 °C until further use.

Characterization. The surface morphology of electrodes was investigated by scanning electron microscopy (SEM) on Hitachi/S-4800. Atomic force microscopy (AFM) was used to study the root-mean square (rms) roughness using Nanonavi E-Sweep. The contact angle measurement was performed on KRUSS/DSA100 by dropping 5 μL deionized water onto the biosensor. Zeta potential was tested using Zeta-sizer Nano ZS instrument (Malvern Instrument UK) by dispersing the materials into deionized water.

Human serum collection. Serum samples were harvested and saved in tubes according to the standard protocol as reported.[25] 3–4 mL of venous blood was injected into a special serum collection tube and overturned up and down for 5–8 times. Then the blood was kept at room temperature for 30 minutes followed by centrifuged at 3500 r min^{-1} for 10 min. All the samples must be transported at 2–8 °C and saved at −80 °C. All of the investigation protocols in this study were approved by the institutional ethics committee School of Biomedical Engineering, Shanghai Jiao Tong University.

Electrochemical detection & ELISA. The whole electrochemical measurements, including differential pulse voltammetry (DPV) and cyclic voltammetry (CV) were performed on a CHI660E electrochemical workstation (Shanghai CH Instruments Co., China) equipped with a Pt indicator electrode, an Ag/AgCl (saturated KCl) reference electrode and an ITO working electrode. The prepared ITO working electrode, indicator electrode, and reference electrode were inserted into the electrochemical cell through the three-electrode holder.[26] The electrodes were dipped in 50 mL of electrolyte consisted 0.5 mM $K_3[Fe(CN)_6]/K_4[Fe(CN)_6]$ and 0.005 M KCl.[27] The DPV curves were conducted from 0.5 V to −0.1 V with a pulse amplitude of 50 mV, a pulse width of 50 ms and a quiet time of 2 s. The CV curves were also conducted from 0.5 V to −0.1 V with a scan rate of 0.01 V s^{-1}, a sweep segment of 2, a sample interval of 0.001 V and a quiet time of 2 s. The ELISA kit was purchased from CUSABIO TECHNOLOGY LLC. All ELISA experiments and data processing were conducted according to the given protocol. Optical density (OD) was measured using BIO-TEK ELX800 and each OD value was obtained as the mean of measurements for 3 times.

Statistical analysis. All statistical analysis in this work was performed on the SPSS software (version 24.0.0.0, IBM SPSS Statistics) to calculate the *p*-value by Independent Student's t-test for statistical demonstration.[1b,28]

Acknowledgements

We gratefully thank the financial support from Projects 81971771, 81771983, 81851110764, 81750110544, 81750410695, and 81650110523 by the National Natural Science Foundation of China, Project YS2017YFGH002082 and 2017YFC0909000 by Ministry of Science and Technology of China, and Innovation Research Plan by the Shanghai Municipal Education Commission (ZXWF082101). This work is also sponsored by the Shanghai Rising-Star Program (19QA1404800) and Changjiang Scholars Program.

Conflicts of interest

The authors declare competing financial interests. The authors have filed patents for both the technology and the use of the technology to detect biosamples.

Keywords: biomarker · electrochemistry · interface · label-free · sensor

[1] a) S. H. Siddiqui, A. Guasconi, J. Vestbo, P. Jones, A. Agusti, P. Paggiaro, J. A. Wedzicha, D. Singh, *Am. J. Respir. Crit. Care Med.* **2015**, *192*, 523;

b) R. Zhang, B. Le, W. Xu, K. Guo, X. Sun, H. Su, L. Huang, J. Huang, T. Shen, T. Liao, Y. Liang, J. X. J. Zhang, H. Dai, K. Qian, *Small Methods* **2019**, *3*, 1800474; c) W. Chen, S. Li, A. S. Kulkarni, L. Huang, J. Cao, K. Qian, J. Wan, *Biotechnol. J.* **2019**, 1900262; d) R. Li, D. D. Gurav, J. Wan, K. Qian, *Precis. Nanomed.* **2018**, *1*, 162; e) J. Wu, X. Wei, J. Gan, L. Huang, T. Shen, J. Lou, B. Liu, J. X. Zhang, K. Qian, *Adv. Funct. Mater.* **2016**, *26*, 4016.

[2] a) D. D. Gurav, Y. Jia, J. Ye, K. Qian, *Nanoscale Adv.* **2019**, *1*, 459; b) C. Rejeeth, X. Pang, R. Zhang, W. Xu, X. Sun, B. Liu, J. Lou, J. Wan, H. Gu, W. Yan, K. Qian, *Nano Res.* **2018**, *11*, 68; c) X. Sun, J. Wan, K. Qian, *Small Methods* **2017**, *1*, 1700196.

[3] a) W. Shu, Y. Wang, C. Liu, R. Li, C. Pei, W. Lou, S. Lin, W. Di, J. Wan, *Small Methods* **2019**, 1900469; b) L. Huang, D. D. Gurav, S. Wu, W. Xu, V. Vedarethinam, J. Yang, H. Su, X. Wan, Y. Fang, B. Shen, C.-A. H. Price, E. Velliou, J. Liu, K. Qian, *Matter* **2019**, https://doi.org/10.1016/j.matt.2019.08.014; c) S. Wu, L. Qian, L. Huang, X. Sun, H. Su, D. D. Gurav, M. Jiang, W. Cai, K. Qian, *Nano-Micro Lett.* **2018**, *10*, 52; d) H. Su, T. Liu, L. Huang, J. Huang, J. Cao, H. Yang, J. Ye, J. Liu, K. Qian, *J. Mater. Chem. B* **2018**, *6*, 7280.

[4] a) L. Tian, J. Qi, X. Ma, X. Wang, C. Yao, W. Song, Y. Wang, *Biosens. Bioelectron.* **2018**, *122*, 43; b) L. P. Jia, R. N. Zhao, L. J. Wang, R. N. Ma, W. Zhang, L. Shang, H. S. Wang, *Biosens. Bioelectron.* **2018**, *117*, 690; c) H. Su, C.-A. Hurd Price, L. Jing, Q. Tian, J. Liu, K. Qian, *Mater. Today Biol.* **2019**, https://doi.org/10.1016/j.mtbio.2019.100033.

[5] a) D. Liu, X. Li, J. Zhou, S. Liu, T. Tian, Y. Song, Z. Zhu, L. Zhou, T. Ji, C. Yang, *Biosens. Bioelectron.* **2017**, *96*, 332; b) B. Viart, C. Dias-Lopes, E. Kozlova, C. F. Oliveira, C. Nguyen, G. Neshich, C. Chavez-Olortegui, F. Molina, L. F. Felicori, *Bioinformatics* **2016**, *32*, 1462.

[6] P. Dobosz, S. Morais, R. Puchades, A. Maquieira, *Biosens. Bioelectron.* **2015**, *69*, 294.

[7] W. D. Lees, L. L. Stejska, D. S. Moss, A. J. Shepherd, *Front. Immunol.* **2017**, *8*, https://doi.org/10.3389/fimmu.2017.00143.

[8] a) X. Wang, S. Li, P. Zhang, F. Lv, L. Liu, L. Li, S. Wang, *Adv. Mater.* **2015**, *27*, 6040; b) C. Wang, R. Hu, J. J. Morrissey, E. D. Kharasch, S. Singamaneni, *Small* **2017**, *13*, 1604255.

[9] G. Sciortino, E. Garribba, J. D. Marechal, *Inorg. Chem.* **2019**, *58*, 294.

[10] a) M. Mathieu, L. Martin-Jaular, G. Lavieu, C. Thery, *Nat. Cell Biol.* **2019**, *21*, 9; b) H. Kawabata, *Free Radical Biol. Med.* **2019**, *133*, 46; c) H. Bu, D. He, X. He, K. Wang, *ChemBioChem* **2019**, *20*, 451.

[11] a) J. Srivastava, A. Kushwaha, M. Srivastava, A. Srivastava, M. Singh, *J. Electroanal. Chem.* **2019**, *835*, 169; b) Y. Wang, K. Qian, K. Guo, J. Kong, J.-L. Marty, C. Yu, B. Liu, *Microchim. Acta* **2011**, *175*, 87.

[12] a) A. Khodadadi, E. Faghih-Mirzaei, H. Karimi-Maleh, A. Abbaspourrad, S. Agarwal, V. K. Gupta, *Sens. Actuators B* **2019**, *284*, 568; b) M. Curtis, H. A. Kenny, B. Ashcroft, A. Mukherjee, A. Johnson, Y. Zhang, Y. Helou, R. Batlle, X. Liu, N. Gutierrez, X. Gao, S. D. Yamada, R. Lastra, A. Montag, N. Ahsan, J. W. Locasale, A. R. Salomon, A. R. Nebreda, E. Lengyel, *Cell Metab.* **2019**, *29*, 141; c) S. Sun, R. Wang, Y. Huang, J. Xu, K. Yao, W. Liu, Y. Cao, K. Qian, *Small* **2019**, *15*, 1902441.

[13] a) S. Zhai, C. Fang, J. Yan, Q. Zhao, Y. Tu, *Anal. Chim. Acta* **2017**, *982*, 62; b) R. Xiong, A. M. Grant, R. Ma, S. Zhang, V. V. Tsukruk, *Mater. Sci. Eng. R* **2018**, *125*, 1; c) F. Gao, F. Zhou, S. Chen, Y. Yao, J. Wu, D. Yin, D. Geng, P. Wang, *Analyst* **2017**, *142*, 4308.

[14] R. Liang, J. Ding, S. Gao, W. Qin, *Angew. Chem. Int. Ed.* **2017**, *56*, 6833; *Angew. Chem.* **2017**, *129*, 6937.

[15] a) P. K. Gupta, N. Pachauri, Z. H. Khan, P. R. Solanki, *J. Electroanal. Chem.* **2017**, *807*, 59; b) H. Sun, D. Li, B. Liu, J. Yao, *Appl. Surf. Sci.* **2019**, *496*, 143680.

[16] a) N. Nikooe, E. Saljoughi, *Appl. Surf. Sci.* **2017**, *413*, 41; b) K. Kubiak-Ossowska, K. Tokarczyk, B. Jachimska, P. A. Mulheran, *J. Phys. Chem. B* **2017**, *121*, 3975.

[17] R. Zhang, C. Rejeeth, W. Xu, C. Zhu, X. Liu, J. Wan, M. Jiang, K. Qian, *Anal. Chem.* **2019**, *91*, 7078.

[18] M. Murphy, K. Theyagarajan, P. Ganesan, S. Senthilkumar, K. Thenmozhi, *Appl. Surf. Sci.* **2019**, *492*, 718.

[19] Z. Bakhtiary, A. A. Saei, M. J. Hajipour, M. Raoufi, O. Vermesh, M. Mahmoudi, *Nanomedicine* **2016**, *12*, 287.

[20] a) M.-L. Næss-Andresen, Å. R. Eggemoen, J. P. Berg, R. S. Falk, A. K. Jenum, *Am. J. Clin. Nutr.* **2019**, *109*, 566; b) J. D. Cook, B. S. Skikne, R. D. Baynes, *Annu. Rev. Med.* **1993**, *44*, 63.

[21] a) J. Guo, X. Gao, L. Su, H. Xia, G. Gu, Z. Pang, X. Jiang, L. Yao, J. Chen, H. Chen, *Biomaterials* **2011**, *32*, 8010; b) B. Liu, Y. Li, H. Wan, L. Wang, W. Xu, S. Zhu, Y. Liang, B. Zhang, J. Lou, H. Dai, K. Qian, *Adv. Funct. Mater.* **2016**, *26*, 7994.

[22] S. Eissa, N. Alshehri, A. M. A. Rahman, M. Dasouki, K. M. Abu-Salah, M. Zourob, *Biosens. Bioelectron.* **2018**, *101*, 282.

[23] D. Dag, S. Guner, M. H. Oztop, *Int. J. Biol. Macromol.* **2019**, *138*, 473.

[24] Y. Deng, W. Wang, L. Zhang, Z. Lu, S. Li, L. Xu, *J. Biomed. Nanotechnol.* **2013**, *9*, 318.

[25] a) X. Wei, Z. Liu, X. Jin, L. Huang, D. D. Gurav, X. Sun, B. Liu, J. Ye, K. Qian, *Anal. Chim. Acta* **2017**, *950*, 147; b) X. Sun, L. Huang, R. Zhang, W. Xu, J. Huang, D. D. Gurav, V. Vedarethinam, R. Chen, J. Lou, Q. Wang, J. Wan, K. Qian, *ACS Cent. Sci.* **2018**, *4*, 223.

[26] a) X. Zhang, J. Li, X. Jia, D. Li, E. Wang, *Anal. Chem.* **2014**, *86*, 5595; b) Y. Lin, P. Yu, J. Hao, Y. Wang, T. Ohsaka, L. Mao, *Anal. Chem.* **2014**, *86*, 3895.

[27] a) L. Jiang, S. Gu, Y. Ding, D. Ye, Z. Zhang, F. Zhang, *Colloids Surf. B* **2013**, *107*, 146; b) A. C. Nielander, A. C. Thompson, C. W. Roske, J. A. Maslyn, Y. Hao, N. T. Plymale, J. Hone, N. S. Lewis, *Nano Lett.* **2016**, *16*, 4082.

[28] a) L. Huang, J. Wan, X. Wei, Y. Liu, J. Huang, X. Sun, R. Zhang, D. D. Gurav, V. Vedarethinam, Y. Li, R. Chen, K. Qian, *Nat. Commun.* **2017**, *8*, 220; b) V. Vedarethinam, L. Huang, W. Xu, R. Zhang, D. D. Gurav, X. Sun, J. Yang, R. Chen, K. Qian, *Small* **2019**, *15*, 1803051.

Manuscript received: October 28, 2019
Revised manuscript received: November 3, 2019
Version of record online: ■■ ▮▮, 0000

COMMUNICATION

*Wanshan Liu, Shiyu Sun, Yida Huang, Ruimin Wang, Jiale Xu, Xiyuan Liu, Kun Qian**

■■ – ■■

Label-Free Detection of Transferrin Receptor by a Designed Ligand-Protein Sensor

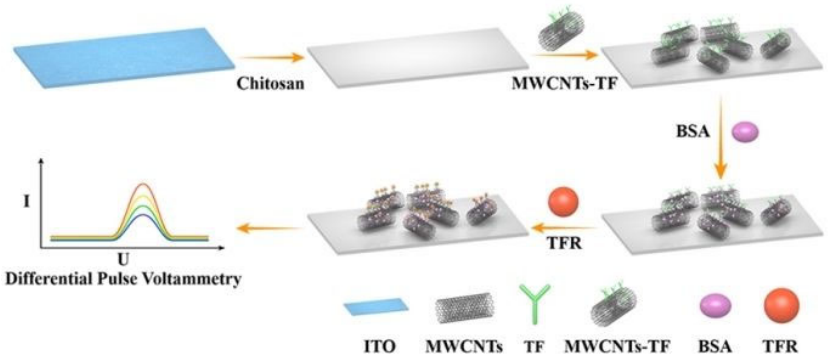

A label-free electrochemical biosensor for transferrin receptor detection is reported that shows a desirable linear range, sensitivity, specificity, reproducibility, and stability for practical applications.